ORIGINAL PAPER

Different morphologies of ZnO nanostructures via polymeric complex sol–gel method: synthesis and characterization

Masoud Farhadi-Khouzani · Zeinab Fereshteh · Mohammad Reza Loghman-Estarki · Reza Shoja Razavi

Abstract Various morphologies of ZnO nanostructures, such as nanoparticles, nanorods and nanoflowers have been achieved controllably by polymeric sol–gel method. In this approach, zinc nitrate $Zn(NO_3)_2 \cdot 6H_2O$, citric acid and ethylene glycol were used as the source of Zn^{2+}, the chelating agent and the solvent agent, respectively. The microstructure of the ZnO nanostructures was characterized by X-ray diffractometry, scanning electron microscopy with the energy dispersive X-ray spectroscopy, transmission electron microscopy, thermogravimetric analysis and Fourier transform infrared spectroscopy. The effect of ethylene glycol to citric acid mole ratio on the morphology and structure of the products was discussed. The ZnO nanoparticles with diameter between 24 ± 2 nm was obtained with EG:CA mole ratio equal to 2:1. The optical properties of as-obtained power were investigated by ultraviolet–visible spectroscopy.

Keywords Nanostructured materials · Polymeric complex method · Semiconductors · Pechini processes · Zinc oxide · Optical properties

M. Farhadi-Khouzani
University of Kashan, Faculty of Chemistry, Kashan, Islamic Republic of Iran

Z. Fereshteh · M. R. Loghman-Estarki (✉)
Department of Materials Engineering, Isfahan University of Technology, Isfahan, Islamic Republic of Iran
e-mail: mr.loghman@ma.iut.ac.ir; loghman57@gmail.com

M. R. Loghman-Estarki · R. S. Razavi
Department of Materials Engineering, Malek Ashtar University of Technology, Isfahan, Shahin-Shahr, Islamic Republic of Iran

1 Introduction

Nanocrystalline semiconductor particles have drawn considerable interest in recent years, because of their special properties, such as large surface-to-volume ratio, increased activity, special electronic properties and unique optical properties as compared to those of the bulk materials. For example, the semiconductor nanocrystals of ZnO, have been extensively studied for their quantum confinement effects and unique size-dependent photoemission properties [1–4]. In this endeavor, scientists have paid a growing attention to the fabrication of materials with specific morphologies because of the expectation of novel properties. For specific applications, a variety of ZnO nano structures have already been fabricated and reported in the literature which include ZnO rods and wires, tubes, belts, propeller, stars, helixes, springs and rings, micro-platelets, nanobridges and nails, columns, hierarchical structures, flower-shaped structures, nano and micro hollow shells, cages and spheres and so on [5–8]. The synthesis approaches include vapor phase evaporation, laser ablation and so forth. However, as the use of these methods involves special equipment complex process control or high temperatures, they are unfavorable for an industrialized process. The chemical methods appear to be of particular interest since they offer the potential of facile scale up, and have flexible processing chemistry. Among chemical methods, sol–gel is an attractive one for preparing nanoparticles because of its easy control, low cost and low fabricating temperature [9, 10]. There are two type of sol–gel [9, 10]: (1) alkoxide gel (2) polymeric gel. In second route, some alpha-hydroxycarboxylic, such as CA, forms polybasic acid chelates with metal cations and then the chelates polymerize with a polyhydroxy alcohol. After calcining the gel, nanometer size powders are achieved. Compared with alkoxide gel, polymeric gel method has better compositional homogeneity, lower toxicity and cost [11, 12].

Here we report synthesis of ZnO nanostructures, prepared by a polymeric complex method using inexpensive starting materials such as zinc nitrate $Zn(NO_3)_2 \cdot 6H_2O$, CA and ethylene glycol used as the source of Zn^{2+}, the chelating agent and the solvent agent, respectively.

2 Experiment

2.1 Materials and physical measurements

All chemical reagents used in our experiments were of analytical grade and were used as received without further purification.

Field emission scanning electron microscopy images were obtained on S-4160 (Hitachi Ltd., Japan). Energy dispersive spectroscopy was obtained with scanning electron microscopy (SERON AIS2300C). Transmission electron microscopy (TEM) micrographs were obtained on a Philips EM208 transmission electron microscope with an accelerating voltage of 100 kV. Samples for TEM were prepared by diluting the product with ethanol and placing a 6 μL drop onto a 200 mesh copper grid covered by a continuous amorphous carbon film. Fourier transform infrared (FT-IR) spectra were recorded on JASCO 680 plus spectrophotometer in KBr pellets. Thermogravimetric analysis (TGA) was carried out using a thermal gravimetric analysis instrument (Malek Ashtar manufacture) with a flow rate of 20.0 mL min^{-1} and a heating rate of 10 °C min^{-1}. XRD patterns (X'Pert Pro, Bruker, Germany) were recorded by a Rigaku D-max C III, X-ray diffractometer using Ni-filtered Cu Kα radiation. In order to investigate optical properties of as-obtained samples, small amount of nanopowder (1 mg) was dispersed in ethanol and from samples ultraviolet–visible (UV–Vis) spectroscopy (Shimadzu UV/3101 PC) was taken in range between 400 and 700 nm. Analysis of particle size was done with the Scion image Beta 4.02 software for image processing.

2.2 Synthesis of ZnO nanostructures

In a typical experiment, 1 mmol $Zn(NO_3)_2 \cdot 6H_2O$ and citric acid (CA) (2 mmol) were dissolved in 100 mL deionized water, and different mole ratios of ethylene glycol (EG) to CA (EG:CA = 2:1, 4:1, 7:1 and 9:1) were then added to form a sol at 50 °C for 1 h. The pH of all precursors was varied in each precursor between $\sim$0.91–2. A white solution was obtained and further heated at 80 °C for 1 h to remove excess water. During continued heating at 150 °C for 1 h, the solution became more and more viscous and finally became a xerogel. To complete drying, xerogel was placed at 250 °C for 1 h. The result powder is a precursor.
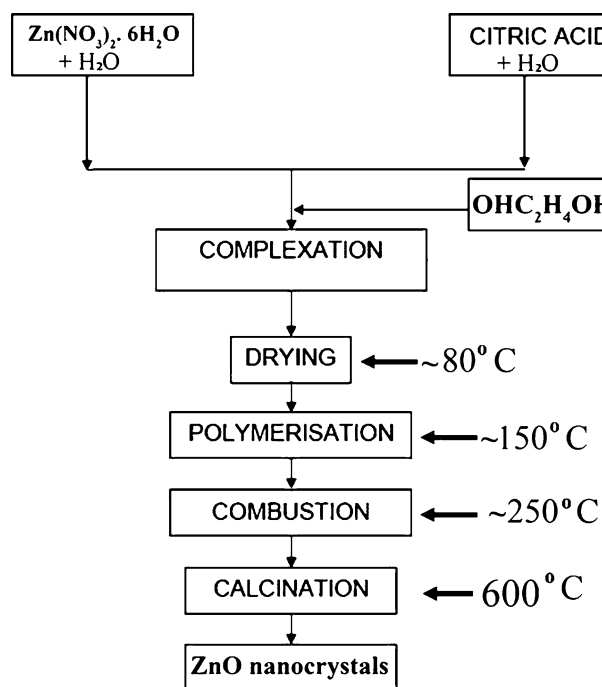

Fig. 1 Preparation of the ZnO nanocrystals

In the furnace, we heat-treated the precursor at 600 °C in air, in a ceramic boat, and then cooled it to reach room temperature. The whole process is summarized in Fig. 1. Number of samples and their corresponding preparations conditions was given at Table 1.

3 Results and discussion

The TGA curve of the samples with different EG–CA mole ratio is shown in Fig. 2. When EG:CA mole ratio were 2:1 (Fig. 2a) TGA profile presented three different stages of decomposition that may be described as follows. The first weight loss that occurred before 300 °C is associated with desorption of physisorbed water and the removal of chemisorbed hydroxyl groups; the second stage occurred over a temperature range of 325–415 °C [13, 14], which can be attributed mainly to the oxidation process of the residual organic materials and the third stage above 510 °C is related to the crystallization of amorphous gel to zinc

Table 1 Number of samples and their corresponding preparations conditions

No.	EG:CA mole ratio	Calcinations temperatures (°C)	Calcinations time (h)
1	2:1	600	2
2	4:1	600	2
3	7:1	600	2
4	9:1	600	2
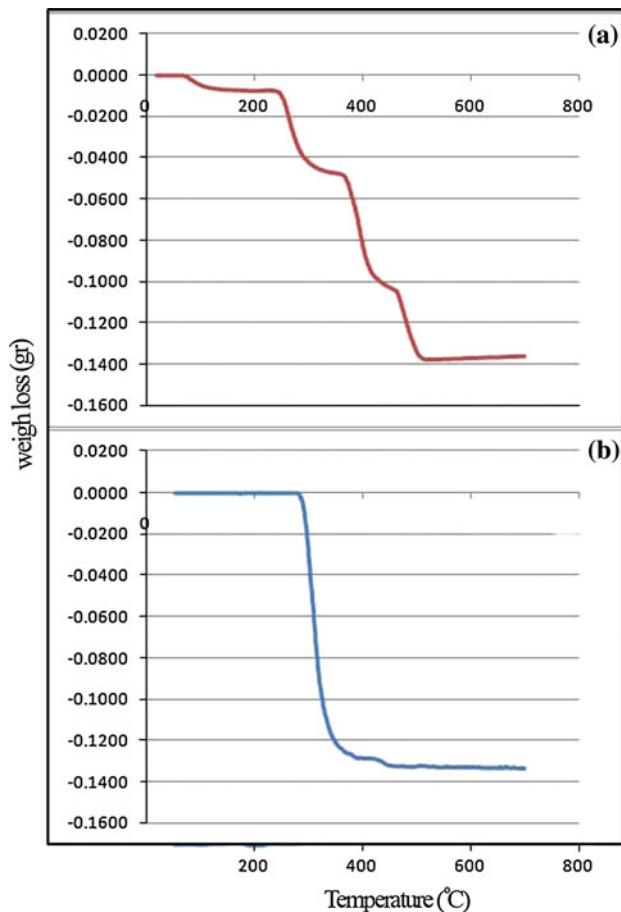
oxide structure [3, 15]. With increasing EG:CA mole ratio to 9:1, most of the organic compounds would be evaporated less than 310°. The weight loss between 310° and 575° can be attributed to crystallizing of amorphous gel to zinc oxide structure [3, 16]. From 600 °C more weight loss was not observed, suggesting the formation of a stable oxide, because zinc oxide nanocrystalline had thermal stability at highest temperatures. These results show the effect of structural stability of ZnO with different EG:CA mole ratio.

Figure 3 shows the XRD patterns of the as-synthesized powders prepared with different EG:CA mole ratio. A search-match data base analysis confirmed all of the products have the phase composition of zincite ZnO with JCPDS card no. 36-1451. The diffraction peaks of (100), (002), and (101) at $2\theta = 32°$, $34.5°$ and $36.4°$ could be distinguished well. Furthermore, no characteristic diffraction peaks arising from the possible impurity phases such as C, $Zn(OH)_2$, etc., were observed, which would indicate the preparation of pure phase ZnO sample by the polymeric complex method.

The effects of the mole ratio EG–CA in the starting solution on the morphology and shape of ZnO powders are
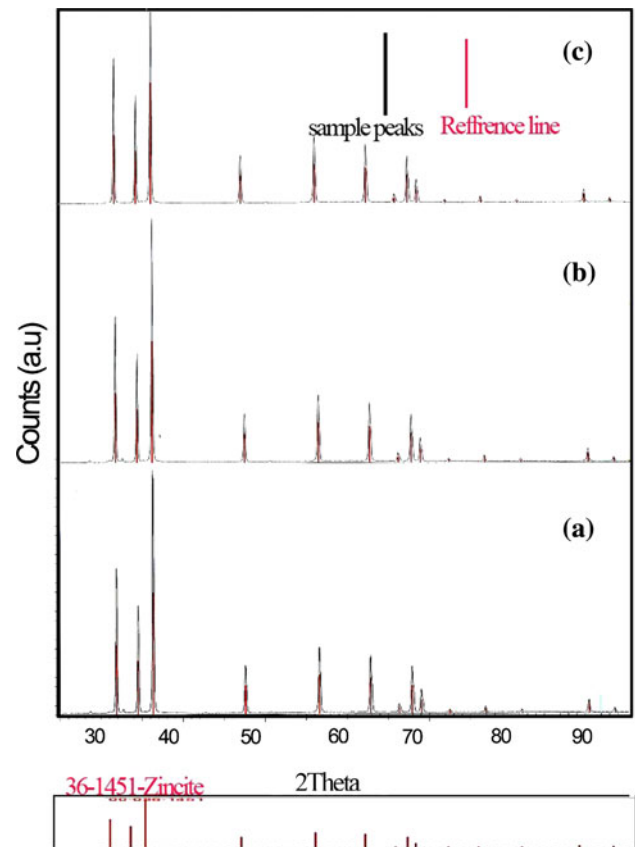
Fig. 3 XRD patterns of ZnO powders obtained with different EG:CA mole ratio **a** 2:1, **b** 4:1 and **c** 9:1

shown in Fig. 4. This figure shows the powder SEM images of the resultant products obtained with EG:CA (2:1–9:1). By increasing EG:CA mole ratio from 2:1 to 9:1, morphologies of the as-synthesized ZnO products can be changed. When EG:CA mole ratio was 2:1, nanoparticles with 25 ± 3 nm diameter were obtained, while in EG:CA mole ratio 4, rod-like samples (Fig. 4b) with average width 400 nm and length up to 10 μm were obtained. It should be noted that, other groups synthesized ZnO nanorods [15–17] with 50–300 nm diameters via sol–gel method. The advantage of present work with aforementioned works is reducing reaction time from 168 h [15] and 28 h [17] to 5 h. Also, we have used less toxic precursors and solvents (water instead of methenamine [16]). This is a key technological achievement for industrial ZnO production. The cross sections of these rods were circular. Upon increasing the mole ratio EG:CA to 7:1, the amount of the rod-like samples with circular cross section in the products decrease as illustrated in Fig. 3c and rod-like ZnO with hexagonal cross section was obtained. The average width and length of these rods were 300–600 nm and more than ~10 μm, respectively. Upon increasing the EG:CA mole ratio to 9:1, the product was found to consist of flower-like ZnO as shown in Fig. 4d. From the SEM image (Fig. 4d) we can
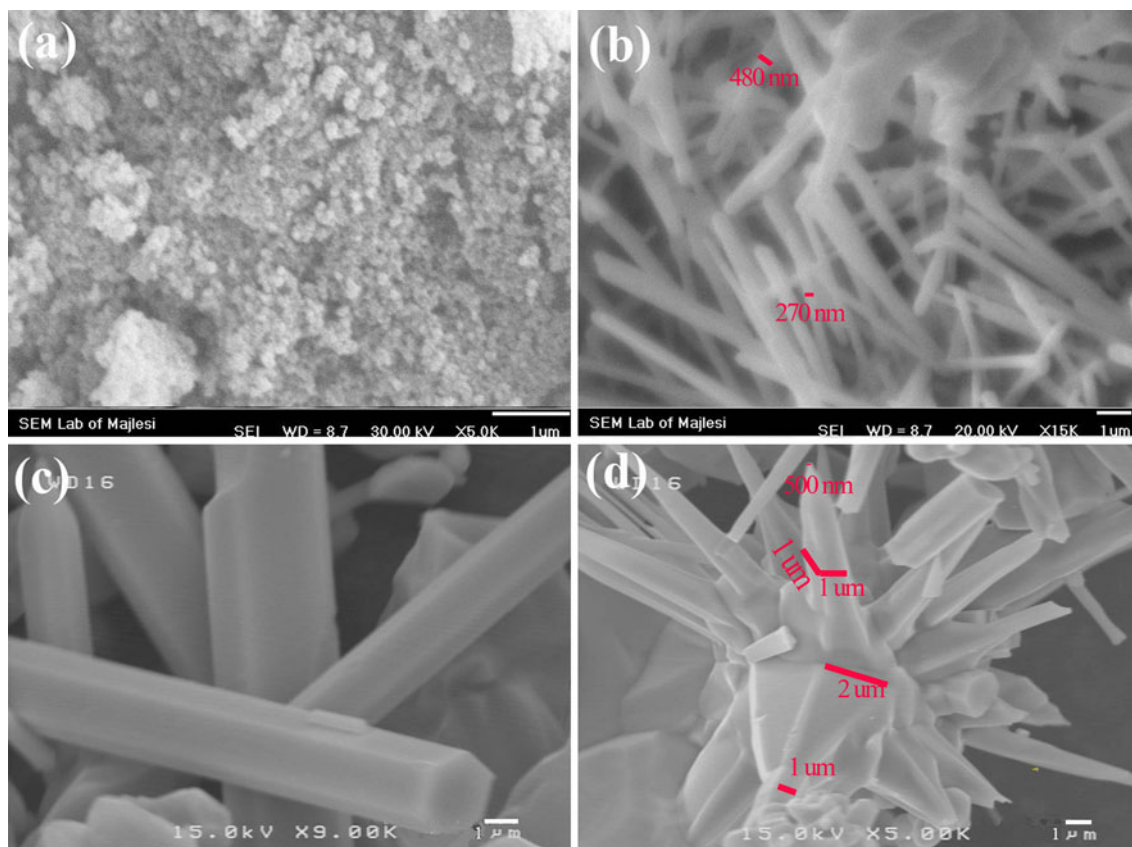
Fig. 4 SEM images of ZnO powders obtained with different EG:CA mole ratio **a** 2:1, **b** 4:1, **c** 7:1 and **d** 9:1

see that the petal in flowers with ~ 500 nm at its top and $\sim 1\ \mu m$ at its bottom and more than 9 μm in length and flowers were built up by sword like ZnO polycrystals.

Typical TEM image of ZnO nanoparticles and nanorods prepared with EG:CA 2:1 and 4:1 are shown in Fig. 5, respectively. Figure 5a shows that the average diameter of nanoparticles is 24 ± 2 nm. According to Fig. 5b, the average width and length of rods are ~ 400 nm and more than 5 μm, respectively.

The energy dispersive X-ray spectroscopy (EDX) analysis of ZnO as-synthesized products with EG:CA mole ratio equal 2:1 are shown in Fig. 6. According to the EDX analysis, the mole ratio oxygen to zinc is 1.01:1, which indicates that there is stoichiometric oxygen in as-grown ZnO crystals.

It should be noted that EDX of all samples approximately resemble the same, so we bring out EDX of ZnO nanoparticles as a typical.

Figure 7 shows the FT-IR spectra of the precursor and the as-synthesized product in the range 500–4,000 cm^{-1}. It should be noted that FTIR of all samples resemble the same, so we bring out FTIR of one sample prepared with EG:CA mole ratio equal 2:1 as a typical. The precursor shows the characteristic absorption bands at about 3,350, 1,400 and 1,360 cm^{-1} corresponding to the –OH group,

NO_3^- ion, and carboxyl group, respectively. In the IR spectrum of the as-synthesized product, there is only one significant spectroscopic band at around 523 cm^{-1}. This is the characteristic band of ZnO [12, 18]. The band at around $\sim 3,343\ cm^{-1}$ is correlated to the hydroxyl group, while the bands at $\sim 1,639$ and $\sim 2,350\ cm^{-1}$ are due to the presence of C=O and CO_2, respectively [12]. The disappearance of the characteristic bands of NO_3^- ion and carboxyl group in the IR spectrum after calcination at 600 °C reveals that the NO_3^- ion and the organic functional groups of CA take part in calcination. Therefore, combustion step in Fig. 1 can be considered as a thermally induced anionic redox reaction of the precursor wherein CA acts as a reductant and the NO_3^- ion acts as an oxidant. Furthermore, it was also found that a light brown gas with pungent smell was released during the initial period of combustion reaction at 250 °C. The gas contains CO_2 and NO_x as identified by escaping gas analysis. Therefore, it is suggested that CA contains carboxyl group, which can be decomposed to produce CO_2 under low temperature. The energy released from the redox reaction, is thus supplied to accelerate the whole combustion reaction. The combination of the lowering of the reaction temperature and the increase in reaction rate results in a combustion reaction of the citric acid–nitrate precursor [10, 11].
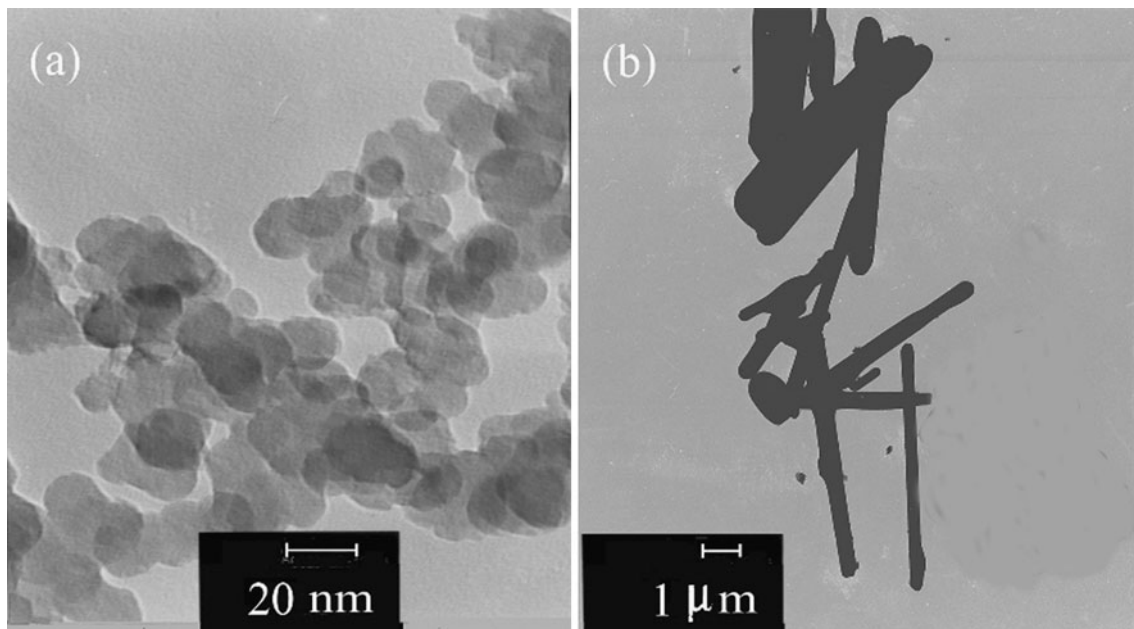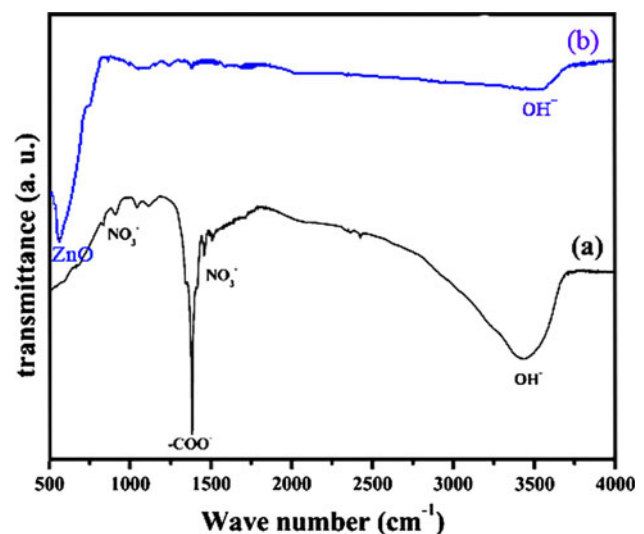
Fig. 5 TEM images of ZnO nanoparticles and nanorods prepared with different EG:CA mole ratio **a** 2:1 and **b** 4:1
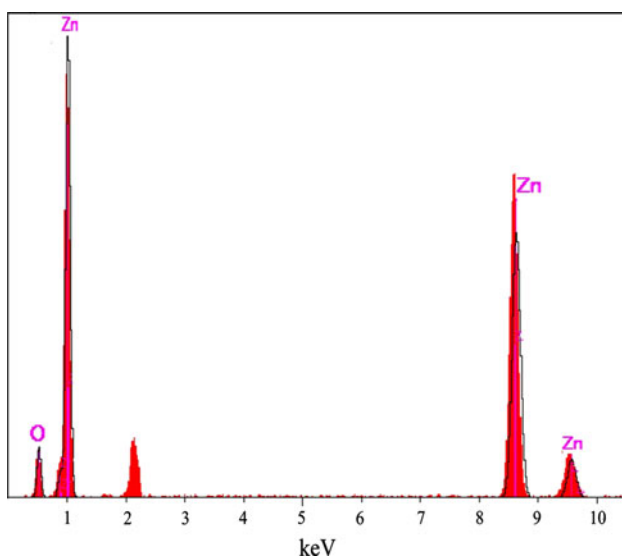
Fig. 6 EDX analysis of ZnO as-synthesized product obtained with EG:CA mole ratio 2:1

Fig. 7 Typical FTIR spectra of the: (*a*) precursor and (*b*) as-synthesized product prepared with EG:CA mole ratio 2:1

The UV–Vis absorption spectra of the ZnO with different morphologies were recorded as shown in Fig. 8. According to Fig. 8, when EG:CA mole ratios were 2:1 and 4:1, the products show a strong absorption edge at about 355, 368 nm, respectively (Fig. 8a, b). Compared with ZnO bulk material, which shows maximum absorption around 375 nm [13, 14], all of the ZnO nanomaterials have shown obvious blue shift due to quantum confinement. Upon increasing EG:CA mole ratio to 9:1 (Fig. 8c), the band edge shifts to 374 nm, which could result from the increase in the mean particle size of ZnO product. By

taking advantage of the optical property difference between ZnO bulk and nanomaterial, it should be possible to apply the ZnO nanomaterials on the UV filter, photocatalysis, and special optical devise.

Polymeric complex method is based on polymerization of metal citrates using EG. Hydrocarboxylic acids such as citric, tartaric and glycolic acids form polybasic acid chelates with metal cations in aqueous solutions. When compared with the majority of acids, CA ($C_3H_4 \cdot (OH) \cdot COOH)_3$) is more widely used in polymeric gel processing because of its high stability. The typical metal complexes with citric ligands tend to be fairly stable due to the strong
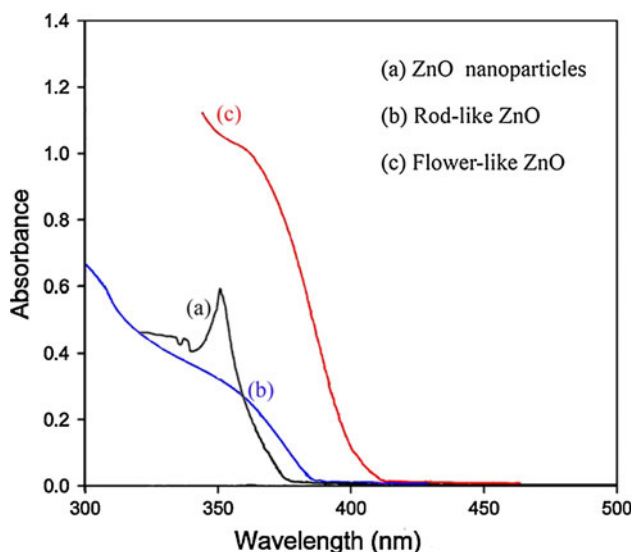
Fig. 8 UV–Vis spectra of ZnO with different morphology: (*a*) nanoparticles, (*b*) nanorods and (*c*) flower-like

coordination of the citric ion with the metal cation involving two carboxyl groups and one hydroxyl group. The addition of a glycol such as EG (OHC_2H_4OH) leads to the formation of an organic ester. Condensation reaction occurs with the formation of a water molecule. The hydroxide ions arise from the carboxylic acid and the protons from the alcohol, generating water molecules. The condensation and polymerization reaction is promoted by heat-treatment [11].

The polymeric precursor method used in this work allowed for obtaining a homogeneous metal-organic polymer in which the zinc ions are, in principle, randomly distributed along the backbone of the polymer. By the heating treatment at 150 °C, this polymeric precursor method goes through two main stages: the first one is the reaction mechanism of esterification of CA with EG, and the second one, the chelation of the zinc acetate by the formed ester as indicated in the previous literature [18–20]. Citric acid and EG generate a reaction of esterification, and the formed ester acts as complexing agent of the zinc cations forming a polymer network that is resin-like or solid as viscosity increases. After calcinations this network ZnO, nanostructures were obtained [11, 20].

Amount of required CA and EG could be calculated by the formula [20, 21]:

$$n = \Sigma(n_i \times v_i) \tag{1}$$

where n_i is charge of cation metal; v_i—number of moles of the metal. In this work, for 1 mmol Zn^{2+} ($n_i = 2$, $v_i = 1$), 2 mmol. CA was used. However, stoichiometric amount of EG reacts to CA molecules to form ester and in continue, with heat treatment, polymeric gel is formed. ZnO exhibits a varied range of novel structures. These structures can be

grown by tuning the growth rates along three fast growing directions:

$\langle 2\bar{1}\bar{1}\rangle(\pm[\bar{1}2\bar{1}0], \pm[2\bar{1}\bar{1}0], \pm[\bar{1}\bar{1}20])$; $\langle 01\bar{1}0\rangle (\pm[01\bar{1}0], \pm[10\bar{1}0], \pm[1\bar{1}00])$ and $\pm[0001]$. The relative surface activities of various growth facets under given conditions determine the surface morphology of the grown structure. Macroscopically, a crystal has different kinetic parameters for different crystal planes, which are emphasized under controlled growth conditions. Thus, after an initial period of nucleation and incubation, a crystallite will commonly develop into a three-dimensional object with well-defined, low-index crystallographic faces. Growth of 1D nanostructures of ZnO was formed by maximizing the areas of the $\{2\bar{1}\bar{1}0\}$ and $\{0\bar{1}\bar{1}0\}$ facets because of the lower energy [6, 22, 23]. With increasing EG:CA mole ratios up to 4:1, extra of EG molecules acts as solvent and linked some facet of initial formed zinc oxide crystals. So, when EG:CA was 2:1, all facets of ZnO grows identically and spherical particles was obtained, while with increasing EG:CA molecules from 2:1 to 4:1 and 9:1, $\{2\bar{1}\bar{1}0\}$ and $\{0\bar{1}\bar{1}0\}$ facets decrease their energy with linking to EG molecules, so morphologies changed to rod and flower like [22, 23]. However suggestion of exact mechanism needs more experiment.

During calcination, the removal of gaseous products from the precursor gives rise to capillary forces on the particles, which brings more particles to come in contact with each other (see the TEM image of samples). This results in more particle agglomeration, cluster formation and particle growth during synthesis [24–26].

Referring to results, we can say that the CA as chelating-fuel agent was added to the solution. It has two different roles in other papers [9, 11]. (1) Citric acid as a chelating agent binds metallic ions (Zn^{2+}) or was applied for formation of complexes for the preparation of zinc oxides, and (2) CA as a fuel helps to progress the synthesis at relatively low temperatures. However, the role of pH in the chemistry of (Zn) gel with different mole ratio of CA to cation has being investigated in our laboratory and their results as soon as would be reported.

4 Conclusion

(1) The ZnO nano structures in rod-like, spherical or flower-like morphologies have been fabricated by a simple polymeric approach with EG:CA mole ratio 2:1, 4:1, 9:1, respectively.

(2) The ZnO nanoparticles with diameter between 24 ± 2 nm were obtained with EG:CA mole ratio equal to 2:1.

(3) XRD analysis confirmed presence of pure ZnO phase and no other phase were observed.

(4) FT-IR spectra showed absorption bands that corresponding to the –OH group, NO^{3-} ion and carboxyl group. In synthesized powder there were only band that is correlated with ZnO. FT-IR spectra illustrated that NO^{3-} ion and organic functional groups of CA take part in calcinations.

(5) During UV–Vis spectroscopy, ZnO absorption spectra of nanopowders prepared with EG:CA mole ratios 2:1, 4:a and 7:1, were shifted toward lower wavelength comparing to bulk ZnO. With increasing EG:CA ratio on 9:1, absorption spectra shifted slightly toward higher wavelength and bandgap of flowerlike ZnO was close to bulk ZnO.

References

1. Xia Y, Yang P, Sun Y, Wu Y, Mare B, Gates B, Yin Y, Kim F, Yan H (2003) Adv Mater 15:323–327
2. Salavati-Niasari M, Davar F, Loghman-Estarki MR (2009) J Alloys Compd 475:782–788
3. Bouropoulos N, Tsiaoussis I, Poulopoulos P, Roditis P, Baskoutas S (2008) Mater Lett 62:3533–3535
4. Salavati-Niasari M, Loghman-Estarki MR, Davar F (2008) Chem Eng J 145:346–350
5. Gao PX, Wang ZL (2003) J Am Chem Soc 125(11299):11305
6. Baruah S, Dutta JD (2009) Sci Technol Adv Mater 10:013 001–0130019
7. Wang ZL (2004) Mater Today 7(26):33
8. He G, Cai JH, Ni G (2008) Mater Chem Phys 110(110):114
9. Salavati-Niasari M, Davar F, Farhadi M (2009) J Sol-Gel Sci Technol 51(48):52
10. Pechini MP (1967) Patent US no. 3 330 697
11. Sakka S, Kozuka H (2005) Handbook of sol–gel science and technology processing, characterization and applications. Kluwer, Dordrecht, pp 60–76
12. Salavati-Niasari M, Davar F, Loghman-Estarki MR (2010) J Alloys Compd 494(199):204
13. Wu L, Wu Y, Lü W (2005) Phys E 28(76):82
14. Zhang YC, Wu X, Hu XY, Guo R (2005) J Cryst Growth 280(250):254
15. Ristić M, Musić S, Ivanda M, Popović S (2005) J Alloys Compd 397:L1–L4
16. Li J, Srinivasan S, He GN, Kang JY, Wu ST, Ponce FA (2008) J Cryst Growth 310(599):603
17. Lee J, Easteal AJ, Pal U, Bhattacharyya D (2009) Curr Appl Phys 9(792):796
18. Shoja Razavi R, Loghman Estarki MR et al (2010) Curr Nano Sci 7:807–812
19. Rani S, Suri P, Shishodia PK, Mehra RM (2008) Sol Energy Mat Sol Cells 92(1639):1645
20. Chezhina NV, Korolev DA (2011) Open Fuel Cells J 4(7):15
21. Shi M, Xu Y, Liu A, Liu N, Wang C, Majewski P, Aldinger F (2009) Mater Chem Phys 114(43):46
22. Liang S, Sheng H, Liu Y, Hio Z, Lu Y, Chen H (2001) J Cryst Growth 225:110
23. Saito N, Haneda H, Sekiguchi T, Ohashi N, Sakaguchi I, Koumoto K (2002) Adv Mater 14:418
24. Sánchez C, Doria J, Paucar C, Hernandez M, Squera AM, Rodríguez JE, Gómez A, Baca E, Morán O (2010) Phys B 405:3679–3684
25. Singh KA, Pathak LC, Roy SK (2007) Ceram Inter 33(1463):1468
26. Mondelaers D, Vanhoyland G, Van den Rul H, Haen JD, Van Bael MK, Mullens J, Van Poucke LC (2002) Mater Res Bull 37(901):914